Electrochemical and Solid-State Letters, **7** (11) A408-A411 (2004)
1099-0062/2004/7(11)/A408/4/$7.00 © The Electrochemical Society, Inc.

Visualization of Liquid Water Transport in a PEFC

X. G. Yang,* F. Y. Zhang, A. L. Lubawy, and C. Y. Wang*,z

Electrochemical Engine Center and Department of Mechanical and Nuclear Engineering, The Pennsylvania State University, University Park, Pennsylvania 16802, USA

Using an optical H_2/air polymer electrolyte fuel cell (PEFC), the mechanics of liquid water transport, starting from droplet emergence on the gas diffusion layer (GDL) surface, droplet growth and departure, to the two-phase flow in gas channels, is characterized under automotive conditions of 0.82 A/cm^2, 70°C, and 2 atm. It is observed that water droplets emerge from the GDL surface under oversaturation of water vapor in the gas phase, appear only at preferential locations, and can grow to a size comparable to the channel dimension under the influence of surface adhesion. Liquid film formation on more hydrophilic channel walls and channel clogging are also revealed and analyzed.
 [DOI: 10.1149/1.1803051]

Manuscript submitted March 3, 2004; revised manuscript received March 23, 2004. Available electronically October 6, 2004.

Water management that balances membrane dehydration with electrode flooding is critical to achieve high performance and longevity of polymer electrolyte fuel cells (PEFCs). At high current density and/or low flow stoichiometry, PEFC is prone to flooding; that is, there is an excessive amount of water accumulated in the cell. If pores in the catalyst layer and gas diffusion layer (GDL) are filled with liquid water, or if the gas channels are clogged by liquid water to such an extent that the transport of reactant gases to the electrodes is hindered, substantially deteriorated cell performance results and mass transport limitation due to flooding occurs. The GDL, either nonwoven carbon paper or woven carbon cloth, is highly porous (>70% with pore sizes in the range of 10-30 μm), electrically conductive, and hydrophobic. In addition, a microporous layer (MPL) (*e.g.*, 30 μm thick), consisting of carbon particles mixed with the PTFE binder, is usually applied onto the side of the GDL facing the catalyst layer. The MPL features a finer pore structure with a pore size on the order of 0.1-0.5 μm. The MPL is intended to provide wicking of liquid water into the GDL by creating a gradient in liquid water pressure and minimize electric contact resistance with the adjacent catalyst layer. Wilson *et al.*[1] speculated that droplets of water generated at the interface of MPL and catalyst layer are in some form proportional in size to the diameter of MPL pores.

Understanding liquid water transport and distribution in a PEFC is a key to unraveling the origin and development of flooding. Prior experimental efforts to probe the water distribution in an operating PEFC have included neutron radiography[2] and gas chromatography (GC)[3,4] measurements. The *in situ* method using neutron radiography was reported to investigate the two-phase flow pattern in the flowfield of both hydrogen and methanol PEFCs. Neutron beams can penetrate through a metal fuel cell to image the real-time liquid water profiles along the large-scale flowfield. However, the neutron radiographic imaging is currently limited in both spatial (*e.g.* >150 μm) and temporal resolution (*e.g.* <30 Hz), making it difficult to capture two-phase flow phenomena in PEFC that is transient in nature and controlled by surface forces. Our previous work[3,4] on water distribution measurement by using a Micro GC provided unique information on the species distributions in both anode and cathode as well as water transport across the membrane. But this diagnostic tool is not applicable to the situation where liquid water is abundant.

Optical diagnostics is capable of investigating the liquid water dynamics in a flooded cell with much higher spatial and temporal resolution. A recent effort has been reported to visualize water buildup in the cathode flowfield of a transparent PEFC operating at low current densities and room temperature.[5] The objective of the present work is to visualize the liquid water transport in a transparent cell under much higher current densities and operating temperatures characteristic of automotive fuel cells. In addition, we describe a series of physical processes leading up to cell flooding, with the aid of an advanced cell design and optical system. These include water droplet emergence from GDL, growth and detachment from GDL, and distribution and removal from the gas channel.

Experimental

The transparent PEFC consisted of a membrane electrode assembly (MEA, 45 μm thick membrane with EW < 1000, 0.4 mg-Pt/cm^2 each electrode) and Toray carbon paper as the GDL [TGPH 090, 20 wt % polytetrafluoroethylene (PTFE) loading] coated with a home-made microporous layer. The MPL was made by coating the slurry of carbon powder Vulcan XC-72 (Cabot) and 20 wt % PTFE onto the carbon paper and then heat-treated at 350°C. The MEA was sandwiched between two gold-plated stainless steel plates acting as current collectors. Before being gold plated, the stainless steel plates (1 mm thick) were machined through to form seven straight gas channels (1 mm wide and 100 mm long), evenly separated by six 1 mm wide lands as current collectors. The resulting cross section of the gas flow channel was 1 × 1 mm, and each gas channel was 100 mm long. The flowfield design for both anode and cathode was identical. The total active area of the test cell was 14 cm^2 defined by gaskets. Two clear polycarbonate plates were placed outside the current collector plates to constrain the gas flow, and two stainless steel end plates compressed the entire optic cell.

Figure 1 shows the experimental setup of the transparent fuel cell. In the present test, pure hydrogen and air were used as the fuel and oxidant with the flow rates of 2.0 A/cm^2 equivalent, or, 0.212 and 0.505 standard L per min (slpm), respectively. The cell pressure was controlled at 2 atm (absolute) for both fuel and air. The cell working temperature and the dew point for fuel and oxidant inlets are described below. All test parameters were computer-controlled by a fuel cell test station (Arbin Instruments, Texas). A Digital camcorder (Sony, DCR VX2000) combined with a microscopy lens (24×) was used to record the microscopic images under proper illumination.

Results and Discussion

Cell performance.—Figure 2 shows several representative I-V polarization curves of the transparent cell under different operation conditions. The cell was preheated by electric heating cartridges up to operation temperatures, *i.e.*, 62 or 70°C, before introducing the humidified fuel/oxidant gases into the cell. At 62°C, both fuel and air gases were supplied at the same stoichiometry of 1 A/cm^2 (or 0.106 and 0.256 slpm, respectively), with dew point of 70°C, resulting in 150% relative humidity (RH) corresponding to 62°C. Here, RH is calculated from the ratio of the saturation pressure at the humidification temperature T to the cell temperature, *i.e.*, $P_T^{H_2O}/P_{T_{cell}}^{H_2O} \times 100\%$. It is seen that the current density reaches 0.74 A/cm^2 at 0.5 V. From its polarization curve shown in Fig. 2, mass transport limitation occurs with current up to 0.75 A/cm^2,

* Electrochemical Society Active Member.
z E-mail: cxw31@psu.edu

Figure 1. Experimental setup of the transparent fuel cell with an active area of 14 cm^2 and seven parallel flow channels on both anode and cathode.

mainly due to low flow rate of oxidant gas (1 A/cm^2 equivalent). The maximum utilization percentage of oxygen in the air is about 80% in this case.

Increasing the cell temperature to 70°C and both stoichiometries of fuel/air gases up to 2 A/cm^2 substantially improves the cell performance. The current density reaches 0.78 A/cm^2 at 0.6 V. The open-circuit voltage (OCV) of the cell at 70°C tests was 0.985 V (its thermodynamic value is ~1.2 V). Using pure oxygen under otherwise identical test conditions, the same cell achieves a mass transport limiting current density of 1.7 A/cm^2, which is translated into 85% utilization of oxygen.

Due to inherently higher electric contact resistances, the present optical cell shows bulk performance close, though inferior to conventional industry cell/stacks. Compared with the transparent cell of Tüber *et al.*,[5] the present cell, however, shows much advantage. Tüber *et al.*[5] built a transparent cell consisting of a Gore-Select PRIMEA MEA with 35 μm thick membrane and standard Toray carbon papers (TGPH-090). Their transparent cell had two straight air channels with an active area of 62 × 6.5 mm, operating at room temperature and ambient pressure with dry fuel and partially humidified air. When the cell was polarized from open circuit to 0.5 V, water accumulation process was chronologically imaged, and the corresponding current was recorded, decreasing from the initial 0.28 to 0.2 A/cm^2 at 3 min after the load due to the partial flooding of the cathode catalyst layer.

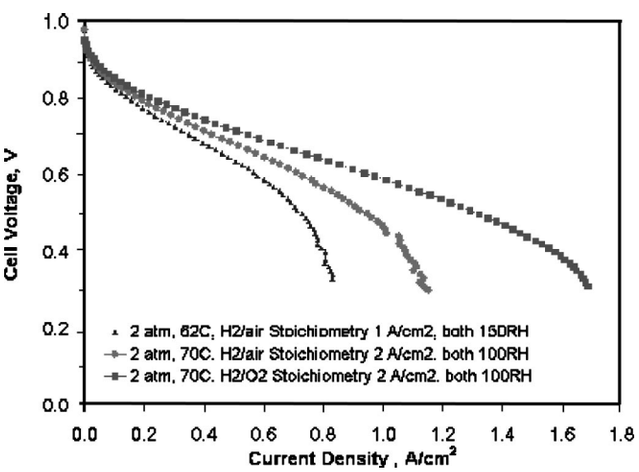

Figure 2. Polarization V-I curves of the transparent hydrogen PEFC, consisting of a membrane electrode assembly (MEA, 45 mm thick membrane, EW < 1000) with a Pt loading of 0.4 mg/cm^2 for each side and Toray TGPH 090 (20 wt % PTFE loading) carbon paper coated with a microporous layer. The cell temperature is 70 or 62°C, and the cell pressure is maintained at 2 atm.

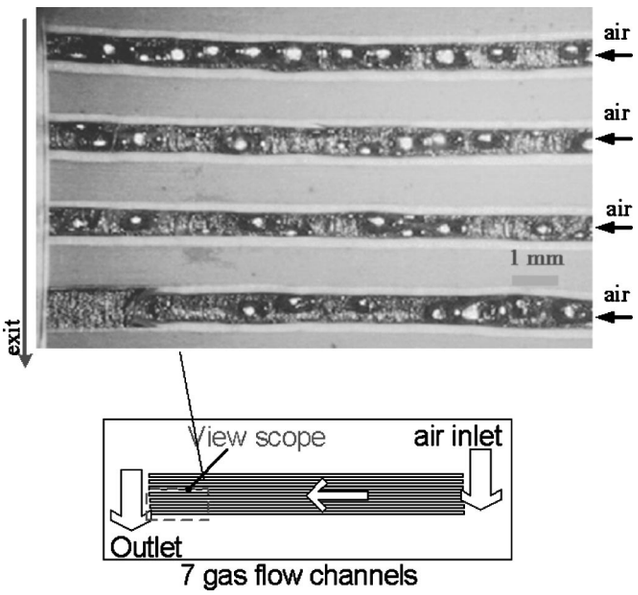

Figure 3. Distribution of water droplets in the region close to the exit.

In comparison, the present cell was designed to allow for optical access under elevated temperature and moist conditions. In addition, the imaging and camera systems used are capable of resolving features down to 10 μm. As generation, interaction, and transport of liquid water vary with the operating current density, temperature, humidification, and gas flow rate, visual results obtained in the present study are expected to be more useful for a basic understanding of flooding mechanisms in automotive fuel cells.

Visualization of liquid water transport.—Visualizations were conducted in the cathode under the following test conditions of 70°C and 2 atm, and the stoichiometry of fully humidified H_2/air fixed at 2 A/cm^2. When the fully saturated gases entered the fuel cell under open-circuit condition, no liquid water condensed from the gas phase could be observed on the GDL surface or along the sidewalls of gas channels. Immediately after switching the cell voltage from the OCV (0.98 V) to 0.40 V, an initial current density of 1.02 A/cm^2 was recorded, and some fog could be seen on the surface of the polycarbonate window. But the fog disappeared in a few seconds. The polycarbonate plate surface was pretreated with a hydrophilic, anti-fog coating so that clear visibility of the gas channel and GDL surface could be achieved even in the hot, moist environment. The current density gradually declined and finally reached 0.82 A/cm^2 in ~5 min under constant voltage of 0.4 V.

Surprisingly, it was observed that hardly any liquid water existed in the upstream section (approximately two-thirds from the cathode inlet) of the gas channels, despite the fact that the inlet gas is fully humidified and the upstream section produces higher current densities.[4] Thus it seems that occurrence of liquid water requires an oversaturated air stream. Quantifying the critical oversaturation for the onset of liquid water is a subject of our ongoing research.

Liquid water started to appear in the last one-third portion of the fuel cell. Figure 3 displays an image of the distribution of water droplets in the steady state operation at 0.4 V, with the view scope of four gas channels focused at a location close to the cathode exit. In this study, the gas flow direction is always from right to left. Droplets of water are randomly scatterred in all channels except for the bottom channel, which was blocked by a water slug. Some droplets of water were able to grow to a size of 0.8 mm in diameter, comparable to the cross-sectional dimension of the flowfield (1 mm wide by 1 mm deep).

A set of close-up images shown in Fig. 4 further delineates the water droplet dynamic process in a gas channel under the same test

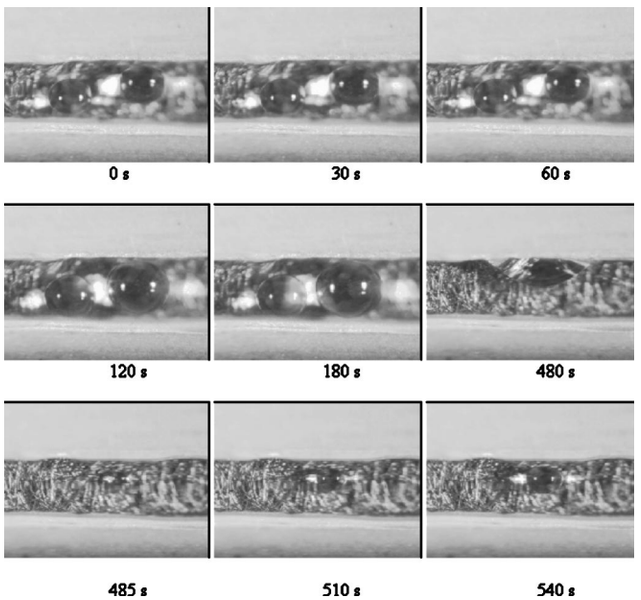

Figure 4. Snapshots of the dynamic process of water droplets in a gas channel at 0.82 A/cm^2 and 70°C. Droplets of water are attached steadily, by surface tension, to the carbon paper. After two droplets coalesce, liquid water is wicked onto the sidewall of the current collecting land at 480 s, where water spreads out and a liquid film is developed. The last three pictures show the re-emergence of a fresh water droplet in the same location on the GDL surface.

conditions as in Fig. 3. The lifetime of these droplets under scope is ~10 min, beginning with emergence and ending at detachment from the GDL surface made of carbon paper. The lifetime of a droplet is determined by the applied current, relative humidity, and velocity of the airflow.

In the first 180 s, Fig. 4 shows two adjacent water droplets growing next to each other. These droplets are attached steadily to the carbon paper under the influence of surface tension. The drag force from the core air flow apparently cannot remove these droplets mechanically. Careful observations further revealed that the growth of water droplets on the GDL surface is an intermittent process, rather than a continuous one, as may be expected. This is because liquid water accumulates somewhere inside GDL to a certain extent, and then is expelled through the opening of the GDL under capillary force to feed surface droplets. Around 480 s after taking the first picture, these two droplets coalesce to form a larger one. Due to its large size, the newly forming droplet immediately touches the upper wall of the gold-plated current collecting land, transforming into a puddle of water, as shown in the picture at 480 s. Finally, the water puddle spreads out along the hydrophilic (gold plated) sidewall, and a liquid film is developed consequently. Under the shear stress of the core air flow, the liquid film is gradually removed toward the channel exit in an annular film flow structure. The last three pictures shown in Fig. 4 show the re-emergence and growth of a fresh droplet at the same opening, indicating that droplets always emerge at preferential locations on the GDL surface. It is believed that these preferential openings are connected to a network of large, hydrophilic pores inside the GDL to form a pathway for liquid water transport.

The process of removing liquid water from the cell can thus be summarized as follows. First, water oozes through the preferential openings of the GDL to nucleate a droplet on the surface. Once it grows big enough to touch the more hydrophilic channel walls, a liquid film is formed as a result of lower surface contact angle. Finally, water gradually migrates along the channel walls toward the exit.

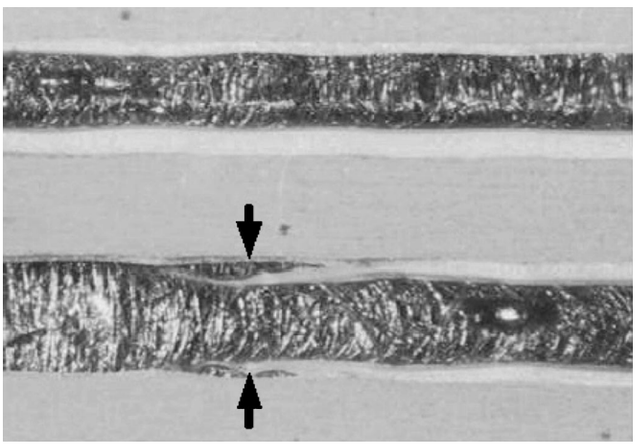

Figure 5. Water films gathering at both sidewalls of the current collecting land symmetrically, showing that gravity is less important than surface tension.

Droplets grown from the GDL surface can be wicked onto either bottom or upper sidewall of the current collector lands, depending upon their emerging locations. In Fig. 4 the droplet of water affixes to the upper sidewall, while Fig. 5 shows the liquid film gathering on both sidewalls symmetrically. The gravitational force is negligible, less by one order of magnitude than surface tension for water droplets with diameters less than 1 mm at 80°C. The ratio of the gravitational force to surface tension is measured by Bond number, defined as $BO = \Delta\rho g d^2/\sigma$, where $\Delta\rho$ is the density difference between liquid and gas, σ the surface tension, d the droplet diameter, g the gravitational acceleration. For this reason, different orientations (vertical or horizontal) of the cell or gas channels are expected to produce only minor effects on liquid water droplet distribution.

The inlet velocity of the humidified air is calculated to be around 0.82 m/s for the air flow of 2 A/cm^2 equivalent. Thus, the gas flow is characterized as low-Reynolds number laminar flow. Under this flow condition, the liquid films thickened and destabilized from the two opposite sidewalls of a gas channel may connect, forming a sealed water band and thereby pinching off the gas flow. This channel clogging by liquid water is shown clearly in Fig. 6. Careful observation indicated that the sealed water band is in a hollow structure. A curving film of water separates the exhaust and inlet gases, pinching off the core gas flow. As a consequence, electrochemical reaction in this channel is shut down, as indicated by the sharp decline in the average current density (Fig. 6b). As the pressure drop across the gas channel is too small to break through the sealed water bridge, the blocked channel will remain idle for quite a long time.

Based on the present observations, it can be concluded that the two-phase flow in the cathode channel with hydrophilic sidewalls (*i.e.*, two gold-plated land surfaces and one surface covered with anti-fog coating) exhibits an annular film flow structure under practical flow stoichiometric ratios. As the gas velocity increases, the two-phase flow pattern may evolve from the annular film flow to mist flow regimes. This is because the high air velocity is able to sweep away water droplets grown from the GDL at a smaller size without having an opportunity to interact with the channel walls. Tests under high stoichiometries (*i.e.*, 5 or 10 A/cm^2 equivalent) could provide direct evidence of the existence of such a mist flow regime. In addition, for industrial fuel cells using graphite bipolar plates, the two-phase flow in gas channels is likely in the form of slug flow as the graphite surface is much less hydrophilic with a contact angle of roughly 70-80°. Work is underway to produce visualization images of this type of flow using a polymer coating to tailor the surface wettability of the transparent fuel cell.

The knowledge of liquid water behaviors on the GDL surface and inside the gas channel, as enabled by the present visualization

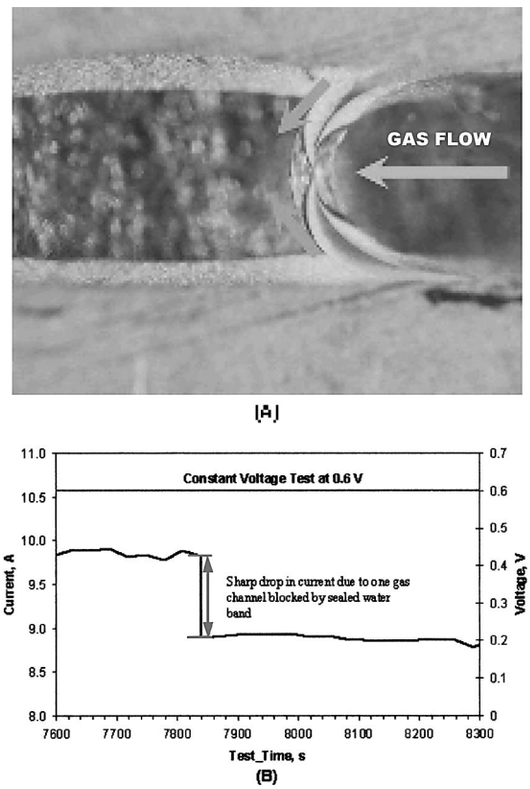

Figure 6. (a) Significant water accumulation to form sealed water band in one of gas flow channels, blocking gas flow and shutting down the cell reaction in this channel, and, consequently, (b) a sharp decline in the cell current at 0.6 V.

technique, provides insight into the liquid water transport and distribution inside the GDL and catalyst layer. As pointed out by Pasaogullari and Wang[6] and several other modeling studies, a decisive parameter to determine the liquid water distribution within GDL is its boundary condition, *i.e.*, the interfacial liquid water coverage. It has been shown that hydrophilic and hydrophobic GDLs both have a similar ability to transport liquid water via capillary forces. The main difference between a hydrophilic and a hydrophobic GDL lies in the liquid water behavior at the GDL/channel interface. The former tends to spread liquid water and hence yield a much higher coverage at the interface, whereas the latter forms discrete droplets as observed in the present study and features a much lower surface coverage by liquid water. Larger interfacial liquid water coverage makes the entire hydrophilic GDL flooded and hence exhibits a distinctive mass transport limitation due to flooding. Work is underway to quantify the interfacial liquid coverage by measuring the droplet detachment diameter and droplet population density as functions of the applied current density, air velocity, and GDL materials.

Conclusion

An advanced transparent fuel cell has been described that can be used to explore liquid water transport in PEFC with high electrochemical performance and good image resolution. In the optical cell, nonuniform water distribution can be found between channels. Liquid water emerges from the GDL surface in the form of droplets with diameters ranging from a few to hundred of micrometers. Droplets of water usually appear and grow at preferential openings on the GDL surface. Surface tension plays a more dominant role than gravitational and air drag forces, holding water droplets firmly on the GDL surface until they grow to a sufficiently large size to touch the more hydrophilic channel walls. Coalescence of water droplets and migration along the hydrophilic surfaces of the gas channel are the main mechanisms of liquid water removal in this transparent fuel cell. If the liquid films grown on channel walls become thick enough to be unstable, a water bridge may form, thereby pinching off the air flow and causing shut-down of the clogged channel. Therefore, it is expected that liquid film drainage from the gas channels is an important topic for flooding avoidance in PEFCs.

Acknowledgments

The authors thank Dr. G. Q. Lu for assistance in the optical cell design and Y. H. Pan for GDL preparation. We also thank Professor K. Sharp for helpful discussions on the design of the imaging system.

The Pennsylvania State University assisted in meeting the publication costs of this article.

References

1. M. S. Wilson, J. A. Valerio, and S. Gottesfeld, *Electrochim. Acta*, **40**, 353 (1995).
2. A. B. Geiger, A. Tsukada, E. Lehmann, P. Vontobel, A. Wokaun, and G. G. Scherer, *Fuel Cells*, **2**, 92 (2002).
3. M. M. Mench, Q. L. Dong, and C. Y. Wang, *J. Power Sources*, **124**, 90 (2003).
4. X. G. Yang, B. Burke, C. Y. Wang, K. Tajiri, and K. Shinohara, To be published.
5. K. Tüber, D. Pócza, and C. Hebling, *J. Power Sources*, **124**, 403 (2003).
6. U. Pasaogullari and C. Y. Wang, *J. Electrochem. Soc.*, **151**, A399 (2004).